Electronic Physician (ISSN: 2008-5842) http://www.ephysician.ir
December 2017, Volume: 9, Issue: 12, Pages: 5932-5939, DOI: http://dx.doi.org/10.19082/5932

Analytical investigation of magnetic field effects on Proton lateral deflection and penetrating depth in the water phantom: A relativistic approach

Mohammad Javad Tahmasebi Birgani[1], Nahid Chegeni[2], Mansour Zabihzadeh[2], Marziyeh Tahmasbi[3]

[1] Ph.D., Professor, Department of Radiation Therapy, Golestan Hospital, Ahvaz Jundishapur University of Medical Sciences, Ahvaz, Iran
[2] Ph.D., Assistant Professor, Department of Medical Physics, Faculty of Medicine, Ahvaz Jundishapur University of Medical Sciences, Ahvaz, Iran
[3] Ph.D. Candidate, Department of Medical Physics, Faculty of Medicine, Ahvaz Jundishapur University of Medical Sciences, Ahvaz, Iran

Type of article: Original

Abstract

Background: Integrated proton therapy - MRI systems are capable of delivering high doses to the target tissues near sensitive organs and achieve better therapeutic results; however, the applied magnetic field for imaging, influences the protons path, changes the penetration depth and deflects the particles, laterally, leading to dose distribution variations.

Objective: To determine the effects of a magnetic field on the range and the lateral deflection of protons, analytically.

Methods: An analytical survey based on protons energy and range power law relation, without using small angle assumption was done. The penetration depth and lateral deflection of protons with therapeutic energy ranges 60-250 MeV in the presence of uniform magnetic fields of 0-10T intensities, were calculated analytically. Calculations were done for relativistic conditions with Mathematica software version 7.0, and MATLAB 7.0 was applied to plot curves and curve fittings.

Results: In the presence of a magnetic field, the depth of Bragg peak was decreased and it was shifted laterally. A second order polynomial model with power equation for its coefficients and a power model with quadratic polynomial coefficients predicted the maximum lateral deflection (y_{max}) and maximum penetration depth (z_{max}) variations with energy and magnetic field intensity, respectively.

Conclusion: The applied correction for deflection angle will give more reliable results in initial energy of 250 MeV and 3T magnetic field intensity. For lower energies and magnetic field intensities the differences are negligible, clinically.

Keywords: Proton radiation therapy, Penetration depth, Lateral deflection, Magnetic field

1. Introduction

Radiation therapy, is one of the main strategies for tumor treatment and control (1). Radiation therapy is done by locating radioactive sources in the patient's body which is called brachytherapy, or by using external sources of ionizing radiation. External sources like photon and high energy electron beams are used for radiation therapy (2, 3). Neutrons and charged particles such as protons, helium and carbon ions, are also used for cancer treatment (2). The final aim of radiation therapy is to apply the highest prescribed dose to tumor, and protect the healthy organs around it (4). The charged particles, due to their Bragg peak, have advantages compared to photon beams with exponential dose deposition and electron beams with their wide area of maximum dose (2, 4-7). A dramatic dose decrease after Bragg peak protects the organs behind the target volume in the radiation therapy (8). Therefore, using protons and heavier charged particles is very desirable for cancer treatment and will give better treatment results. Although, the

Corresponding author:
Marziyeh Tahmasbi, Department of Medical Physics, Faculty of Medicine, Jundishapur University of Medical Sciences, Ahvaz, Iran. Tel: +98.9163026244, Email: marziyeh_tahmasbi@yahoo.com
Received: July 23, 2017, Accepted: September 12, 2017, Published: December 2017
iThenticate screening: September 01, 2017, English editing: October 26, 2017, Quality control: November 12, 2017
This article has been reviewed / commented by five experts

associated equipment is complex and expensive (4, 9-11). Also, geometry and characteristics of the beam path through the body are important in charged particle therapy treatment planning. Therefore, determining the exact location of tumor and dose localization in charged particle therapy is serious (12). Today, online tumor tracking and image guided radiation therapy by magnetic resonance imaging are developed as a promising approach for this task (12-15). As the magnetic field can affect the charged particles according to Lorentz equation (Eq. 1) and deflect their path in the medium (16):

$$F = qvBsin\theta \qquad (1)$$

The applied magnetic fields in the integrated radiation therapy-MRI systems can alter the lateral deflection and penetration depth of the charged particles in radiation therapy (12-15), which are responsible for dose dispositioning in the patient's body (8). Therefore, the influences of these changes on the dose distributions in the target volume should be noticed. On the other hand, the concern of producing hot and cold spots in target volume due to the applied magnetic fields and the necessitation of treatment planning modifications have been indicated in literature (13-14, 17-21). Also, for spreading out the Bragg peak to cover the whole volume of the target in proton therapy, modulators are used in the beam path which leads to neutron contamination (22-23). Another approach is the use of a magnetic field, which reduces neutron contamination (24-25). As, the magnetic field can deflect the charged particles path and change the location of their Bragg peak (26), investigating the effects of magnetic fields on charged particle therapy, is important. Some literature has discussed the effects of the magnetic field on proton path in the water. Fuchs et al. presented a fast numerical method for particle beam dose calculation in the presence of a magnetic field (17). Sardari et al. applied a transverse static magnetic field for in vivo proton beam shaping, and found an increase in tumor dose of about 30-90% and a decrease in the dose of healthy tissue about 10% (26). Raaymakers et al. found that a 0.5 T magnetic field can only deflect the proton beam about 1 and 2 mm in a water phantom and patient's body, respectively (27). Schippers and Lomax found an 8mm deflection for a 200 MeV proton beam in a 0.5 T magnetic field (28). Oborn et al. results showed a large deflection of beam in a direction perpendicular to the magnetic field lines (29). Wolf and Bortfeld found that the maximum lateral deflection of particles at the end of their range is proportional to the third power of their initial energy (30). Schellhammer and Hoffmann predicted the trajectory of a mono-energetic proton beam in water phantom in the presence of a transverse magnetic field for repositioning the Bragg peak to its intended location (31). All of the reviewed literature revealed the necessitation of considering Bragg peak movement due to magnetic fields in treatment calculations, even for small magnetic field intensities or low proton energies. Since the magnetic field alters the penetration depth and deflects the particles laterally, it can change dose distributions in treatment planning (30). For increasing dose calculation precision, magnetic field effects should be considered in dose calculations (17). Using Monte Carlo based simulation methods are often too time-consuming to calculate these changes. So, researchers are still interested in continuing to apply the analytical methods and to improve them in the future (32). Standard analytical models can be used in modern treatment planning for particle therapy dose calculations (17). Therefore, providing an analytical relationship for lateral deflection and penetrating depth of protons with magnetic field intensity can be useful for dosimetry and therapeutic proposes. In most of the previous analytical and numerical studies (30, 31), small angle approximation has been applied to calculate deflection angle of protons in the presence of the magnetic field, while the deflection angle is not small enough to use this approximation. Therefore, this study aims to propose a simple and more accurate analytical method to calculate the penetration depth and lateral deflection of protons with different initial energies in a water phantom in the presence of a magnetic field of different intensities by considering relativistic conditions without small angle assumption.

2. Material and Methods

This study is done analytically based on power law range- energy relationship as follows:

$$R_0 = \alpha E_0^p \qquad (2)$$

Where $\boldsymbol{R_0}$ and $\boldsymbol{E_0}$ are the range and initial energy of the protons, respectively (30, 33). The parameter α is a material-dependent constant, and p takes into account the dependence of the proton's energy or velocity (33). In our calculations, the parameters α and p are assumed to be $\boldsymbol{2 \cdot 43 \times 10^{-3}}$ and 1.75, respectively (30). The energy of protons at depth z (E(z)) can be expressed as (33):

$$\boldsymbol{E(z) = (\frac{R_0 - z}{\alpha})^{\frac{1}{p}}} \qquad (\boldsymbol{3})$$

Consider a mono energetic proton beam traveling along the z-axis and a static magnetic field of different strengths applied in the x –axis direction perpendicular to the particles path (z), the proton beam will take a curvature path (s) in the medium due to the magnetic field and Lorentz force (Figure 1). Therefore; to calculate E as a function of the distance travelled s, the Eq. 3 can be rewritten for s instead of z. The radius of the curvature path r (s) of proton in the magnetic field is as follows:

$$r(s) = \frac{m \cdot \gamma(s) \cdot v(s)}{q \cdot B} \qquad (4)$$

Where m is the mass of proton travelling along z-axes and passing through a static magnetic field (B) applied across the x-axes, v(s) and q are the velocity and the charge of proton, respectively. Lorentz factor ($\gamma(s)$) equals $1/\sqrt{1-(v/c)^2}$ as a relativistic factor. Since the length of the partial curvature path of proton in the medium, ds, can be approximated by multiplying the curvature radius r and the deflection angle d$\emptyset$ ($ds = r(s)d\emptyset(s)$) according to (30) and Eq.4, it can be written as:

$$d\emptyset = \frac{qB}{\sqrt{2mE(s)(1+\frac{E(s)}{2mc^2})}}ds \qquad (5)$$

The total deflection angle,$\emptyset(s)$ is measured by integrating the distance s which the proton has travelled.

$$\int_0^{\emptyset(s)} d\emptyset(s') = \int_0^s \frac{qB}{\sqrt{2mE(s')(1+\frac{E(s')}{2mc^2})}}ds \qquad (6)$$

This integration requires the functional form of E(s) obtained from Eq. 3. In this study, using Mathematica software version7.0, the Tailor series expansion of $1/\sqrt{2mE(s')(1+\frac{E(s')}{2mc^2})}$ with 6 terms was obtained and then the deflection angle $\emptyset(s)$ was calculated. Finally, the lateral deflection of protons in y direction was calculated with regard to $y(s) = \int_0^s sin\emptyset(s')ds'$. Also, the penetration depth of proton in z direction was determined by $z(s) = \int_0^s cos\emptyset(s') \cdot ds'$. In most of the previous studies (30), small angle approximation has been applied to calculate y(s) and z(s), while the deflection angle is not small enough to use this approximation. Therefore, employing Mathematica, y(s) and z(s), were calculated by 7 terms Tailor series expansion; however, due to their large size, the extracted equations for y(s) and z(s) are not included in the article. For initial energies, 60-250 MeV, the magnetic field intensity (B) was changed from zero to 10T. The maximum lateral deflection y_{max} (cm) and the penetration depth z_{max} (cm) of protons were calculated and tabulated for each magnetic field intensity B(T) and various initial energies under relativistic conditions (not been shown). To investigate the effect of magnetic field intensity (B (T)), the y_{max} and z_{max} were plotted for each initial energy under relativistic conditions. In addition, the variations of y_{max} and $z_{max,}$ were drawn as a function of initial energy for different magnetic field intensities finally, variations of the maximum lateral deflection and penetration depth of protons with the magnetic field intensity and initial energy were formulated using curve fitting toolbox in MATLAB version7.

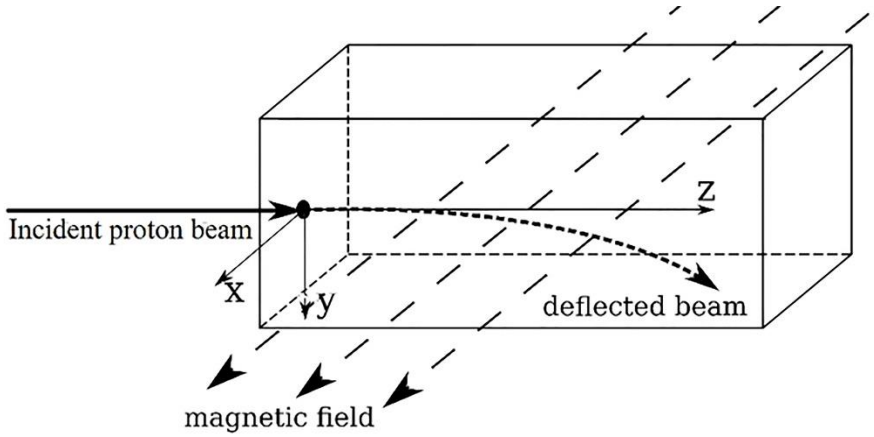

Figure 1. Schematic illustration of the supposed geometry. The continuous arrow marks the initial beam direction, while the direction of beam deflection is shown by a dotted line. The dashed arrows indicates the magnetic field orientation which is perpendicular to the initial direction of protons (adapted from Ref. 17- modified for the assumed geometry).

3. Results

The calculated maximum lateral deflection y_{max} and penetration depth z_{max} of protons, for each initial energy in the presence of magnetic field is shown in Figure 2-a, b. variations of y_{max} and $z_{max,}$ in cm, were drawn as a function of initial energy (MeV) for different magnetic field intensities (Tesla) in Figure 2-c, d.

The quadratic polynomial model was used to formulate the maximum lateral deflection regarding magnetic field intensity (data shown in Figure 2-a) as follows:

$$y_{max}(B) = \alpha B^2 + \beta B + \gamma \qquad (7)$$

Where the fitting parameters α, β and γ for different initial energies are shown in Table 1 with $R^2 > 0.99$.
Since the parameters α, β and γ are initial energy related, applying a power model has revealed the best fit (R^2>0.99) as follows:

$$y_{max}(B,\ E_0) = a_1 {E_0}^5\ B^2 + a_2 {E_0}^{3.17} B + a_3 {E_0}^{4.6} \qquad (8)$$

Where a_1, a_2 and a_3 are -1.42×10^{-13}, 1.03×10^{-7} and -2.78×10^{-12}, respectively.
For maximum penetration depth, the power model predicted its variations with initial energy (data shown in Figure 2-d) as follows:

$$z_{max}(E_0) = \mathrm{a}\ {E_0}^b \qquad (9)$$

Where the fitting parameters a, b are shown for different magnetic field intensities in Table 2 with R^2> 0.97. As shown in Table 2, the parameters a, b are related to magnetic field intensity (B). The best fit was obtained by employing a quadratic polynomial model with R^2>0.98 as follows:

$$\mathrm{z_{max}}(\mathrm{E_0}, \mathrm{B}) = (\mathrm{a_1 B^2 + a_2 B + a_3}) {E_0}^{(b_1 \mathrm{B^2 + b_2 B + b_3})} \qquad (10)$$

Where a_1, a_2, a_3, b_1, b_2 and b_3 are 0.001, -0.004, 0.005, -0.004, -0.43 and 1.79, respectively.

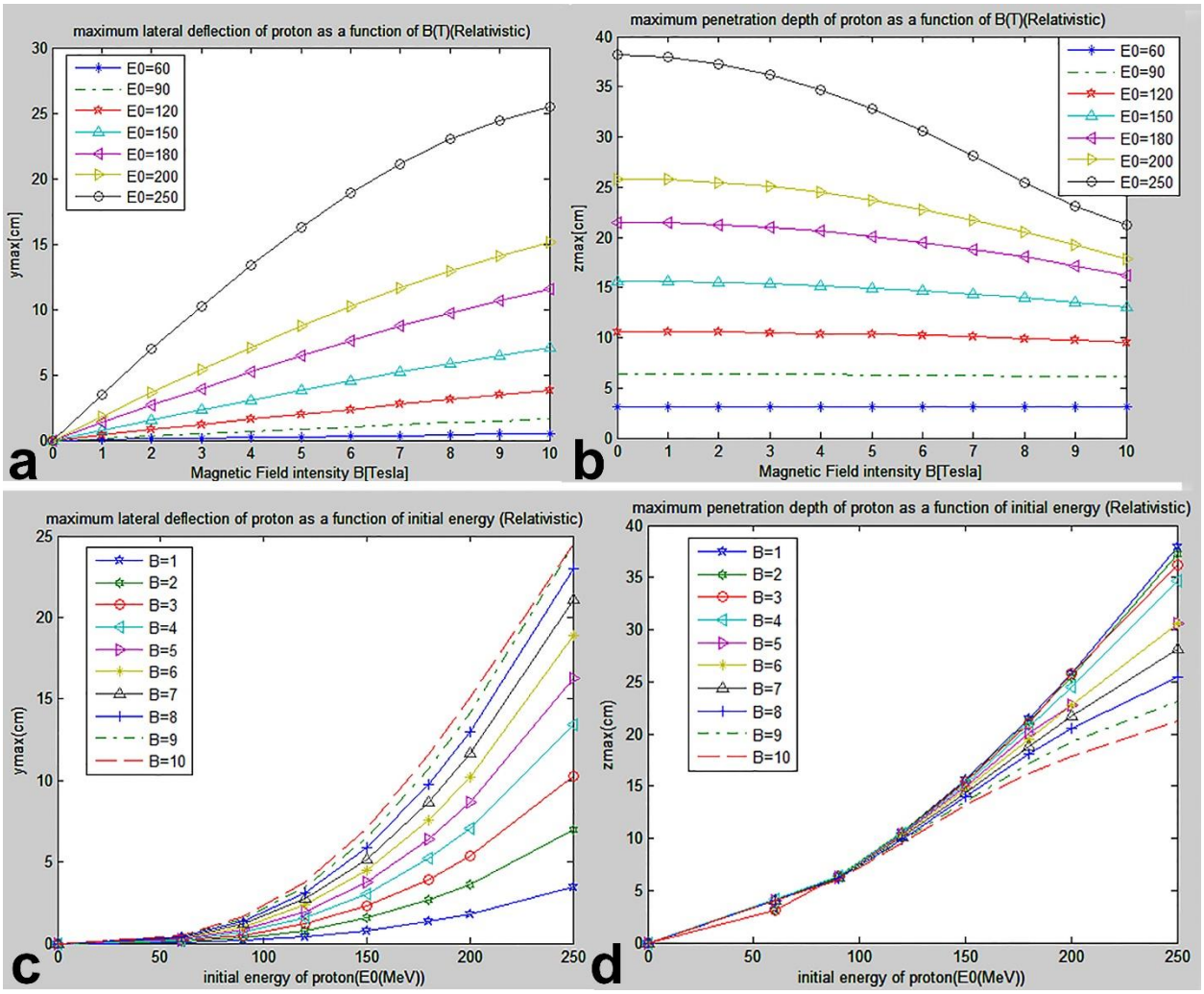

Figure 2. a) The maximum lateral deflection (y_{max}) and b) the maximum penetration (z_{max}) of protons with different initial energies in the presence of magnetic field in water. c) the maximum latral deflection (y_{max}) and d) the maximum penetration depth (z_{max}) of protons in the presence of magnetic field as a function of initial energy.

Table 1. The fitting parameters α, β and γ for different initial energies of proton in the fitted quadratic polynomial model to the variations of proton maximum lateral deflection with magnetic field intensity changes $y_{max}(B)= \alpha B^2+ \beta B+ \gamma$.

E_0(MeV)	α	β	γ
70	0.00	0.08	0.00
90	0.00	0.17	0.00
120	0.00	0.41	- 0.01
150	- 0.01	0.81	- 0.02
180	- 0.03	1.43	- 0.06
200	- 0.05	1.98	- 0.10
250	- 0.14	4.02	- 0.30
300	- 0.35	7.19	- 0.67

Table 2. The parameters of the fitted power model for maximum penetration depth of proton z_{max} (cm) as a function of E_0 (MeV) ($z_{max}(E_0)= a E_0^{b}$).

B(T)	0	1	2	3	4	5	6	7	8	9	10
a	0.0024	0.0025	0.0030	0.0040	0.0054	0.0084	0.0144	0.0242	0.0368	0.0513	0.0663
b	1.75	1.74	1.71	1.65	1.58	1.49	1.38	1.27	1.18	1.10	1.04

4. Discussion

Advantages of the proton therapy such as Bragg peak, dramatic distal dose decrease, multiple scattering, lateral dose fall off, and localized dose provide more accuracy in dose delivery to tumors near sensitive organs (34, 35). To achieve these benefits, identifying factors like geometry, characteristics, density of beam path, and tumor position is essential in treatment planning systems for hadron therapy (12). This issue necessitates integrating proton therapy facilities with magnetic resonance imaging systems (MRI) which makes possible radiation therapy based on real time imaging of soft tissue. MRI can determine tumor variations during radiotherapy to modify treatment planning between dose delivery fractions (13, 19). However, the applied magnetic field can alter proton range and lateral deflection, which consequently changes dose distribution (14, 19). As shown in Figure 2, for therapeutic protons with energy in the range of 60-250 MeV, the maximum lateral deflection at the end of the range in the presence of a magnetic field had an increasing trend with increasing magnetic field intensity while maximum penetration depth was reduced. According to Figure 2-a, 2-c, the maximum lateral deflection showed a rising trend with increasing magnetic field intensity and the initial energy of protons. A second order polynomial model was fitted to the maximum lateral deflection and magnetic field intensity with $R^2 > 0.99$, where polynomial coefficients had a power relation with the initial energy (Table 1), which leads to a general formula calculating y_{max} as a function of E_0 and B (Eq. 8). As seen, the lateral deflection of protons in the presence of a magnetic field was a function of initial energy and magnetic field intensity. By substituting the initial energy of protons in MeV and the magnetic field intensity in Tesla, in Eq. 8, the maximum lateral deflection of protons will be achieved in cm. As shown in Figure 2-b, the maximum axillary projected range or the so-called maximum penetration depth of protons (z_{max}) reduced with increasing magnetic field intensity. This was due to proton deviation which caused protons to traverse a curvature path in the medium and lose more energy. As illustrated in Figure 2-d, the maximum penetration depth (z_{max}) increased with energy. A power model with $R^2>$ 0.97, was applied to maximum penetration depth of proton and initial energy relation in water (Eq.9), whose coefficients (Table 2), were related to magnetic field intensity by quadratic polynomials equation. Finally, z_{max} was achieved as a function of E_0, and B (Eq.10). By substituting the initial energy of protons in MeV and the magnetic field intensity in Tesla, the maximum penetration depth of protons will be calculable in cm. By applying the acquired equations (Eq. 8, 10), fast and accurate calculation of lateral deflection and penetration depth of proton beams with different initial energies will be possible in the presence of a magnetic field of any intensity. The comparison of the presented method with other researchers was illustrated in Tables 3 and 4. Generally, Table 3 and 4 indicated good agreement with the results of previous studies (17, 30-31). As Schellhammer and Hoffmann (31) mentioned, the small angle approximation in the clinical energy range for calculating lateral deflection and penetration depth of protons in the presence of magnetic field intensities below 3 Tesla did not have considerable effects in the results. Data in Tables 3 and 4 indicated this fact, too. On the other hand, Wolf and Bortfeld (30) presented an analytical method by assuming the small angle approximation for calculating the beam deflection and we did not apply small angle assumption, but the results showed good agreement. According to Tables 3 and 4, the presented results without small angle approximation, were closer to those of Schellhammer and Hoffmann (31), in initial energy of 250 MeV and 3T magnetic field intensity. Because, Schellhammer and Hoffmann (31) had improved the Wolf and Bortfeld model (30)

for rotation radius and deflection angle. For lower energies and magnetic field intensities the differences are negligible, clinically. In clinical treatment planning systems, the analytical methods are faster than Monte Carlo based approaches to calculate dose distributions in the presence of the uniform magnetic field. Moreover, while the calculation of Bragg peak deflection will be faster using Eq.8, 10, the restrictions of this method compared to Monte Carlo methods are not considering the secondary particles, inhomogeneity of medium and non-uniformity of magnetic field.

Table 3. Comparison of predicted lateral deflection (y_{max}) of a mono energetic proton beam with initial energy E_0 (MeV) at the Bragg peak in relativistic condition. The beam passes through a water phantom in a uniform magnetic field of B (T).

Y_{max} (mm)								
B (T)	E0 (MeV)	Proposed method	Wolf & Bortfeld (30)[I]	Fuchs et al. (17)[II]	Schellhammer &Hoffmann (31)[III]	%D* with I	%D* with II	%D* with III
0.35	60	0.18	0.20	0.20	0.20	-11.11	-11.11	-11.11
	150	2.71	2.70	2.50	2.70	0.37	7.75	0.37
	250	12.30	12.40	11.80	12.40	-0.81	4.06	-0.81
0.5	90	0.86	0.90	-	0.90	-4.65	-	-4.65
	200	9.08	9.20	-	9.20	-1.32	-	-1.32
1.0	60	0.50	0.50	0.50	0.50	0.00	0.00	0.00
	150	7.73	7.80	7.30	7.80	-0.91	5.56	-0.91
	250	35.05	35.50	32.80	35.40	-1.28	6.42	-1.00
1.5	90	2.53	2.60	-	2.60	-2.77	-	-2.77
	200	27.14	27.50	-	27.40	-1.33	-	-0.96
3	60	1.51	1.50	1.40	1.50	0.66	7.28	0.66
	90	5.06	5.20	-	5.10	-2.77	-	-0.79
	120	11.90	12.10	-	-12.00	-1.68	-	-0.84
	150	23.03	23.50	22.80	23.20	-2.04	0.74	-1.00
	180	39.39	40.30	-	39.70	-2.31	-	-0.79
	200	53.64	55.10	-	-	-2.72	-	-
	250	102.61	106.60	98.90	103.40	-3.89	3.62	-0.77

I: Analytical method, II: Simulation method, III: Iterative analytical method, %D*: the percent of relative differences between our proposed method and other studies.

Table 4. Comparison of predicted penetration depth variations (Δz_{max} in mm) of a mono energetic proton beam with initial energy E_0 (MeV) at the Bragg peak in relativistic condition. The beam passes through a water phantom in a uniform magnetic field of B (T).

Δz_{max} (mm)					
B (T)	E_0 (MeV)	Proposed method	Wolf & Bortfeld (30)[I]	Fuchs et al. (17)[II]	Schellhammer &Hoffmann (31)[III]
0.35	60	0.00	0.00	0.83	0.00
	150	0.00	0.00	0.23	0.00
	250	0.28	0.30	6.96	0.30
1.0	60	0.01	0.00	0.83	0.00
	150	0.26	0.30	1.23	0.30
	250	2.24	2.60	8.95	2.30
3	60	0.05	0.10	0.93	0.10
	120	0.90	1.00	-	1.00
	150	2.40	2.60	3.23	2.50
	180	5.10	5.70	-	5.30
	250	19.92	23.10	25.94	20.70

I: Analytical method, II: Simulation method, III: Iterative analytical method

5. Conclusions

The proposed analytical approach can predict the deflection and penetration depth of a proton beam in the presence of a magnetic field of any intensity, which can be a fast and accurate method for calculating the variation of dose

distribution in MRI-based proton therapy treatment planning systems and research. Applying a magnetic field of suitable and enough intensity perpendicular to the proton beam path can force the proton to go through a spiral path inside the target volume, which, consequently, increases the dose in the target volume sparing the organs behind it, which is ideal in hadron therapy. But, this is an initial proposal in proton therapy and may not be applicable in a clinical situation to concentrate the dose in the target volume, because magnetic fields with high intensities will be needed to do this, and these intensities cannot be applied to the patient's body. Although, they can be used in simulation environments or in vitro experiments.

Acknowledgments:
This research was supported by the Vice-Chancellor for Research of Jundishapur University of Medical Science, Ahvaz, Iran, for financial support with grant number (U-94176). We thank Dr. Jalalvand for sharing his experiences about Mathematica software. We would also like to show our gratitude to Dr. Rahmani for comments that greatly improved the language of the manuscript.

Conflict of Interest:
There is no conflict of interest to be declared.

Authors' contributions:
All authors contributed to this project and article equally. All authors read and approved the final manuscript.

References:

1) Price P, Sikora K. Treatment of Cancer. 5th ed. London: Arnold Hodder; 2008.
2) Chu WT, Ludewigt BA, Renner TR. Instrumentation for treatment of cancer using proton and light-ion beams. Rev Sci Instrum. 1993; 64(8): 2055-2122. doi: 10.1063/1.1143946.
3) Brahme A. Design Principles and Clinical Possibilities With a new Generation of Radiation Therapy Equipment. Acta Oncologia. 1987; 26(6): 403-12. doi: 10.3109/02841868709113708. PMID: 3328620.
4) Khan Fhaiz M. the physics of the radiation therapy. 4th ed. Wolters Kluwer Health; 2010.
5) Hollmark M, Uhrdin J, Belkic Dz, Gudowska I, Brahme A. Influence of multiple scattering and energy loss straggling on the absorbed dose distribution of therapeutic light ion beams: I. Analytical pencil beam model. Phys Med Biol. 2004; 49(14): 3247-65. doi: 10.1088/0031-9155/49/14/016.
6) Scifoni E, Surdutovich E, Solov'yov A, Pshenichnov I, Mishustin I, Greiner W. Ion-beam therapy: from electron production in tissue like media to DNA damage estimations. Biological Physics. 2008; 104: 104-10. doi: 10.1063/1.3058968.
7) DePauw N, Dias MF, Rosenfeld A, Seco JC. Ion Radiography as a Tool for Patient Set-up & Image Guided Particle Therapy: A Monte Carlo Study. Technology in Cancer Research & Treatment. 2014; 13(1): 69-79. doi: 10.7785/tcrt.2012.500357.
8) You S, Gou Ch, Wu Zh, Hou Q. A semi-analytical model for calculating the penetration depth of a High energy electron beam in a water phantom with a magnetic field. Physica Medica. 2015; 31(5): 463-7. doi: 10.1016/j.ejmp.2015.04.013.
9) Schulte R, Bashkirov V, Li T, Liang Zh, Mueller K, Heimann J, et al. Conceptual Design of a Proton Computed Tomography System for Applications in Proton Radiation Therapy. IEEE Transaction On Nuclear Science. 2004; 51(3): 866-72. doi: 10.1109/TNS.2004.829392.
10) Pedroni E, Bacher R, Blattmann H, Böhringer T, Coray A, Lomax A, et al. The 200 MeV proton therapy project at the Paul Scherrer Institute: Conceptual design and practical realization. Medical Physics. 1995; 22(1): 37-53. doi: 10.1118/1.597522.
11) Pedroni E. Latest Development in Proton Therapy. Proceedings of EPAC 2000, Vienna, Austria.
12) Riboldi M, Orecchia R, Baroni G. Real-time tumour tracking in particle therapy: technological developments and future perspectives. The lancet oncology. 2012; 13(9): 383-91. doi: 10.1016/S1470-2045(12)70243-7.
13) Vander Heide UA, Houweling AC, Groenendaal G, Beets-Tan RGH, Lambin Ph. Functional MRI for radiotherapy dose painting. Magn Reson Imaging. 2012; 30(9): 1216-23. doi: 10.1016/j.mri.2012.04.010.
14) Raaymakers BW, Raaijmakers AJE, Kotte ANTJ, Jette D, Lagendijk JJW. Integrating a MRI scanner with a 6MV radiotherapy accelerator: dose deposition in a transverse magnetic field. Phys Med Biol. 2004; 49(17): 4109–18. doi: 10.1088/0031-9155/49/17/019.
15) Keyvanloo A, Burke B, Warkentin B, Tadic T, Rathee S, Kirkby C, et al. Skin dose in longitudinal and transverse linac-MRIs using Monte Carlo and realistic 3D MRI field models. Med Phys. 2012; 39(10): 6509-21. doi: 10.1118/1.4754657. PMID: 23039685.

16) Haliday D, Resnick R, Walker J. fundamentals of physics extended. Wiley; 2010.
17) Fuchs H, Moser P, Groschl M, Georg D. Magnetic field effects on particle beams and their implications for dose calculation in MR guided particle therapy. 2017.
18) Bol GH, Issoiny SH, Lagendijk JJW, Raaymakers BW. Fast online Monte Carlo-based IMRT planning for the MRI linear accelerator. Phys Med Biol. 2012; 57(5): 1375–85. doi: 10.1088/0031-9155/57/5/1375.
19) Yang YM, Geurts M, Smilowitz JB, Sterpin E, Bednarz BP. Monte Carlo simulations of patient dose perturbations in rotational-type radiotherapy due to a transverse magnetic field: A tomotherapy investigation. Med Phys. 2015; 42(2): 715-25. doi: 10.1118/1.4905168.
20) Ghila A, Fallone BG, Rathee S. Influence of standard RF coil material on surface and build up dose from a 6 MV photon beam in magnetic field. Med Phys. 2016; 43(11): 5808-16. doi: 10.1118/1.4963803. PMID: 27806597.
21) Chen X, Prior P, Chen G, Schuitz CJ, Li XA. Technical Note: Dose effects of 1.5 T transverse magnetic field on tissue interfaces in MRI- guided radiotherapy. Med Phys. 2016; 43(8): 4797-802. doi: 10.1118/1.4959534. PMID: 27487897.
22) Paganetti H, Jiang H, Trofimov A. 4D Monte Carlo simulation of proton beam scanning: modelling of variations in time and space to study the interplay between scanning pattern and time-dependent patient geometry. Phys Med Biol. 2005; 50(5): 983–90. doi: 10.1088/0031-9155/50/5/020.
23) Koehler AM, Schneider RJ, Sisterson JM. Flattening of proton dose distribution for large field radiotherapy. Medical Physics. 1977; 4(4): 297- 301. doi: 10.1118/1.594317.
24) Bues M, Newhauser WD, Titt U, Smith AR. Therapeutic step and shoot proton beam spot-scanning with a multi-leaf collimator: a Monte Carlo study. Radiation Protection Dosimetry .2005; 115(1–4): 164–9. doi: 10.1093/rpd/nci259.
25) Bjerke HH. Application of Novel Accelerator Research for Particle Therapy. 2014.
26) Sardari D, Hosseini-hamid M, Saeidi P. In-vivo Proton Beam Shaping Using Static Magnetic Field for Cancer Therapy. World Congress on Medical Physics and Biomedical Engineering. Munich, Germany. 2009; 25(1): 949-51. doi: 10.1007/978-3-642-03474-9_266.
27) Raaymakers BW, Raaijmakers AJ, Lagendijk JJ. Feasibility of MRI guided proton therapy: magnetic field dose effects. Phys Med Biol. 2008; 53(20): 5615-22. doi: 10.1088/0031-9155/53/20/003.
28) Schippers JM, Lomax AJ. Emerging technologies in proton therapy. Acta Oncol. 2011; 50(6): 838-50. doi: 10.3109/0284186X.2011.582513.
29) Oborn BM, Dowdell S, Metcalfe PE, Crozier S, Mohan R, Keall PJ. Proton beam deflection in MRI fields: Implications for MRI-guided proton therapy. Med Phys. 2015; 42(5): 2113-24. doi: 10.1118/1.4916661.
30) Wolf R, Bortfeld T. An analytical solution to proton Bragg peak deflection in a magnetic field. Phys Med. Biol. 2012; 57(17): 329–37. doi: 10.1088/0031-9155/57/17/N329.
31) Schellhammer SM, Hoffmann AL. Prediction and compensation of magnetic beam deflection in MR-integrated proton therapy: a method optimized regarding accuracy, versatility and speed. Phys Med Biol. 2017; 62: 1549-64. doi: 10.1088/1361-6560/62/4/1548. PMID: 28121631.
32) Schaffner B, Pedroni E, Lomax A. Dose calculation models for proton treatment planning using a dynamic beam delivery system: An attempt to include density heterogeneity effects in the analytical dose calculation. Phys Med Biol. 1999; 44: 27–41. doi: 10.1088/0031-9155/44/1/004. PMID: 10071873.
33) Bortfeld T. An analytical approximation of the Bragg curve for therapeutic proton beams. Med Phys. 1997; 24(12): 2024-33. doi: 10.1118/1.598116. PMID: 9434986.
34) Newhauser WD, Zhang R. The physics of proton therapy. Phys Med Biol. 2015; 60: 155–209. doi: 10.1088/0031-9155/60/8/R155. PMID: 25803097, PMCID: PMC4407514.
35) Schulz-Ertner D, Tsujii H. Particle Radiation Therapy Using Proton and Heavier Ion Beams. J Clin Oncol. 2007; 25(8): 953-64. doi: 10.1200/JCO.2006.09.7816. PMID: 17350944.